ACADEMIA ROMÂNĂ
Revue Roumaine de Chimie
https://www.icf.ro/rrch/

Rev. Roum. Chim.,
2023, *68*(9), 419–427
DOI: 10.33224/rrch.2023.68.9.02

QUANTITATIVE STRUCTURE-ACTIVITY RELATIONSHIP FOR THIAZOLIDINE-2,4-DIONE DERIVATIVES AS INHIBITORY ACTIVITIES OF 15-PGDH USING MLR AND ANN

Sihem MEDJAHED,[a,b] Salah BELAIDI,[b,*] Noureddine TCHOUAR,[a] Houmam BELAIDI,[b] Fatima SOUALMIA[a] and Samir CHTITA[c]

[a]Laboratory of Process and Environmental Engineering (LIPE), Faculty of Chemistry, University of Science and Technology of Oran Mohamed Boudiaf, USTO-MB, BP 1503, El M'naouer, 31000 Oran, Algeria
[b]Group of Computational and Pharmaceutical Chemistry, Laboratory of Molecular Chemistry and Environment, Department of Chemistry, University of Biskra, BP 145 Biskra 07000, Algeria
[c]Laboratory of Physical Chemistry of Materials, Faculty of Sciences Ben M'Sik, Hassan II University of Casablanca, BP7955 Sidi Othmane, Casablanca, Morocco

Received June 5, 2021

Quantitative structure activity relationship studies were applied on a series of 22 molecules of thiazolidine-2,4-dione. The compounds used are potent inhibitors of the 15-hydroxyprostaglandin dehydrogenase (15-PGDH). The present study was performed using multiple regression analysis (MLR) and artificial neural network (ANN) to predict a QSAR model using molecular descriptors. Our results suggest QSAR model based of the following descriptors: polarizability (Pol), molar volume (MV), hydration energy (HE), surface area grid (SAG), molar weight (MW), energy of frontier orbital's E_{HOMO} (The Highest Occupied Molecular Orbital) and E_{LUMO} (The Lowest Unoccupied Molecular Orbital) and atomic net charges (q_{N3}, q_{C4}, q_{C5} and q_{O7}) for the inhibitory activities of 15-hydroxyprostaglandin dehydrogenase. The best predictive models by MLR and ANN methods gave highly significant square correlation coefficient (R^2) values of 0.9623 and 0.9963 respectively. The model also exhibited good predictive power confirmed by the high value of R^2_{pred} (0.7839 and 0.6324 respectively).

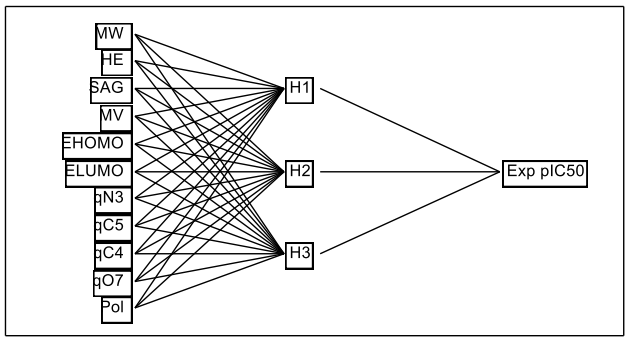

INTRODUCTION

Thiazolidine-2,4-dione derivatives have been studied extensively and found to have diverse chemical reactivity.[1–3] Thiazolidine derivatives displayed a broad spectrum of biological activities including antimicrobial,[3,4] antidiabetic,[5,6] antiobesity,[7] anti-inflammatory,[8] antioxidant,[9] antiproliferative,[10] and antitumor.[11] They inhibit corrosion of mild steels in acidic solution.[12] Density functional theory methods offer an alternative use of inexpensive computational methods, which could handle relatively large molecules.[13–17]

* Corresponding author: s.belaidi@univ-biskra.dz, prof.belaidi@gmail.com

The kind of activity is a function of the user's[18] interest. QSAR is a predictive tool for a preliminary evaluation of the activity of chemical compounds by using computer aided models.[19–21]

Quantitative structure activity relationship techniques increase the probability of success, reduce time, and cost in the drug discovery process.[22–25] QSAR has done much to enhance our understanding of fundamental processes and phenomena in medicinal chemistry and drug design.[26–29]

Multiple linear regression (MLR) is a mathematical tool that quantifies the relationship between a dependent variable and one or more independent variables, it was used to develop QSAR models and all the variables that have been included in the model are significant.[30–37]

Neural networks are artificial systems; they use a large number of interrelated data-processing neurons to emulate the function ofthe brain.[38]

The primary route of prostaglandin metabolism in the body is initiated by 15-Hydroxyprostaglandin Dehydrogenase (15-PGDH), which oxidizes the hydroxyl group to the ketogroup at position 15.[39]

Such a process leads to a pronounced loss of biological activity, making it a key enzyme for prostaglandin biological inactivation.[40] It inactivates a number of active leukotrienes and hydroxyeicosatetraenoic acids (HETEs). 15-PGDH can be found in many mammalian tissues especially the lung, kidneys and placenta[41]. Inhibition of 15-PGDH enzyme has drawn great attention in clinical management to reduce hair loss[42], gastric ulcer healing,[43] bone formationand interestingly dermal wound healing.[44]

In the current study, we applied the QSAR for the prediction of thiazolidine-2,4-dione derivatives with inhibition of 15-PGDH activities.

MATERIALS AND METHODS

In the present work, the inhibition of 15-PGDH,[45] by a group of thiazolidine-2,4-dione derivatives was investigated to predict a QSAR model using molecular descriptors and (ANN, MLR) analysis. A group of 22 thiazolidine-2,4-dione (Fig. 1) derivatives inhibitors of 15-hydroxyprostaglandin dehydrogenase (15-PGDH) was selected for the study. The reported IC_{50} values (M) have been converted to the logarithmic scale [pIC_{50}], for QSAR study.

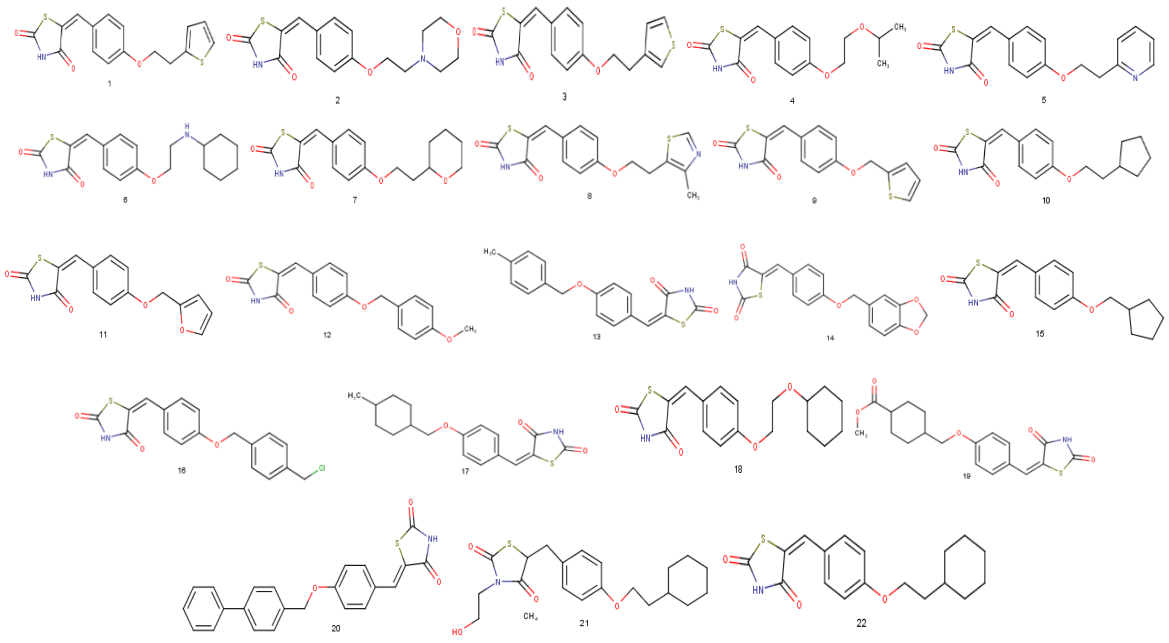

Fig. 1 – 2Dstructures of thiazolidine-2,4-dione derivatives.
These derivatives of thiazolidine-2,4-dione were synthesized by Y. Wu *et al.* 2010, and these structures were designed by *MarvinSketch 6.2.1* software.

Firstly, the twenty-three investigated molecules were preoptimized using the Molecular Mechanics, with Force Field (MM+) included in *HyperChem* version (8.08) package.[46] After that, the results fromoptimized structures were further refined using the semi-empirical *PM3* Hamiltonian implemented

also in *HyperChem*. We chose a gradient norm limit of 0.01 kcal/Å for the geometry optimization.

The QSAR properties module from *HyperChem* (8.08) was used to calculate: molar polarizability (Pol), partition coefficient octanol/water (log*P*), molar volume (MV), hydration energy (HE), surface area grid (SAG) and molar weight (MW).

The Quantum Chemical descriptors: energy of frontier orbital's E_{HOMO} and E_{LUMO} and atomic net charges (q_{S1}, q_{N3}, q_{C4}, q_{C5}, q_{O6} and q_{O7}) were computed using *Gaussian 09W* software[47] by using DFT/B3LYP with cc-pVDZ basis set.[25]

We used the software JMP 8.0.2[48] for multiple linear regression analysis and artificial neural network of molecular descriptors.

RESULTS AND DISCUSSION

Structure activity relationship (SAR)

An important objective of this study was to evaluate the physicochemical domain on twenty-two derivatives of thiazolidine-2, 4-dione (Fig. 1) concerning their 15-PGDH inhibitors activity. The present series of thiazolidine-2, 4-dione derivatives have been synthesized and characterized by Y. Wu *et al.*[45]

The properties involved are: surface area grid (SAG), molar volume (MV), hydration energy (HE), partition coefficient octanol/water (log*P*), polarizability (Pol) and molecular weight (MW), the charges, the Highest Occupied Molecular Orbital (E_{HOMO}) and the Lowest Unoccupied Molecular Orbital (E_{LUMO}), which are listed in Tables 1 and 2. The results were calculated using *HyperChem8.0.8* and *Gaussian09* software.

The molecular polarizability of a molecule characterizes the capability of its electronic system to modulate itself on the application of external fields, and it plays an important role in modeling many molecular properties and biological activities.

Table 1

Values of physicochemical descriptors used in the regression analysis

Compound	MW (uma)	HE (kcal/mol)	Log P	SAG ($A°^2$)	Pol ($A°^3$)	MV ($A°^3$)
1	331.4000	-8.2000	-0.8100	542.5900	34.8200	890.7500
2	334.3900	-7.5100	-0.8500	559.9100	34.1900	925.0600
3	331.4000	-8.3200	-0.7000	541.4000	34.8200	892.5300
4	307.3600	-6.7200	0.1100	558.3900	31.7800	900.4000
5	326.3700	-8.4600	0.4900	551.8500	34.5900	907.8900
6	346.4400	-6.9600	0.7200	616.3400	37.2300	1013.6400
7	333.400	-6.1600	0.2000	578.4400	34.6800	945.3300
8	346.4200	-8.3500	-1.3500	555.9900	35.9500	925.1400
9	317.3800	-8.7600	-0.8600	517.4800	32.9800	838.0600
10	317.4000	-4.6200	1.3400	563.3500	34.0400	920.5500
11	301.3200	-10.2400	-1.2000	507.5500	30.6200	816.0400
12	341.3800	-9.5900	-0.4600	564.8100	35.9400	941.3300
13	325.3800	-6.7800	0.6800	553.0000	35.3000	913.9900
14	355.3600	-12.0200	-1.2700	566.4900	35.8000	930.8600
15	303.3800	-5.0200	1.0200	532.4200	32.2000	869.7200
16	359.8300	-7.0300	0.8300	581.4700	37.2300	960.9200
17	331.4300	-4.5500	1.7500	573.1400	35.8700	954.5600
18	347.4300	-6.0800	0.9400	606.4500	36.5100	1001.0200
19	375.4400	-7.3700	0.7800	623.8200	38.4300	1041.9100
20	387.4500	-8.8200	1.1400	633.3700	43.1200	1069.8600
21	375.4800	-8.1500	1.5400	649.6300	40.1800	1090.1600
22	331.4300	-4.7300	1.7400	579.4700	35.8700	961.0500

Table 2

Values of quantum descriptors used in the regression analysis

Compound	E_{HOMO} (a.u)	E_{LUMO} (a.u)	qS1	qN3	qC4	qC5	qO6	qO7
1	-0.2199	-0.0806	0.2450	-0.7050	0.7130	-0.3000	-0.5610	-0.5870
2	-0.2109	-0.0793	0.2440	-0.7050	0.7120	-0.3010	-0.5620	-0.5880
3	-0.2202	-0.0809	0.2450	-0.7050	0.7130	-0.3000	-0.5610	-0.5870
4	-0.2191	-0.0793	0.2460	-0.7050	0.7130	-0.3000	-0.5620	-0.5880
5	-0.2179	-0.0790	0.2440	-0.7050	0.7120	-0.3010	-0.5620	-0.5880
6	-0.2180	-0.0785	0.2450	-0.7050	0.7120	-0.3010	-0.5620	-0.5880
7	-0.2170	-0.0782	0.2450	-0.7050	0.7120	-0.3010	-0.5620	-0.5890
8	-0.2217	-0.0821	0.2450	-0.7050	0.7130	-0.2990	-0.5610	-0.5870
9	-0.2193	-0.0792	0.2460	-0.7050	0.7130	-0.3000	-0.5620	-0.5880
10	-0.2176	-0.0786	0.2450	-0.7050	0.7120	-0.3010	-0.5620	-0.5880
11	-0.2187	-0.0789	0.2450	-0.7050	0.7120	-0.3010	-0.5620	-0.5880
12	-0.2170	-0.0775	0.2450	-0.7050	0.7120	-0.3010	-0.5630	-0.5890
13	-0.2179	-0.0782	0.2460	-0.7050	0.7120	-0.3010	-0.5630	-0.5880
14	-0.2176	-0.0785	0.2460	-0.7050	0.7120	-0.3010	-0.5620	-0.5880
15	-0.2171	-0.0784	0.2440	-0.7050	0.7120	-0.3010	-0.5620	-0.5880
16	-0.2204	-0.0800	0.2480	-0.7050	0.7130	-0.2990	-0.5610	-0.5870
17	-0.2181	-0.0787	0.2450	-0.7050	0.7120	-0.3010	-0.5620	-0.5880
18	-0.2193	-0.0794	0.2460	-0.7050	0.7130	-0.3000	-0.5620	-0.5880
19	-0.2188	-0.0793	0.2450	-0.7050	0.7120	-0.3000	-0.5620	-0.5880
20	-0.2190	-0.0791	0.2470	-0.7050	0.7130	-0.3000	-0.5620	-0.5880
21	-0.2164	-0.0769	0.2560	-0.5610	0.7180	-0.2940	-0.5700	-0.5960
22	-0.2178	-0.0784	0.2450	-0.7050	0.7120	-0.3010	-0.5620	-0.5880

Solvent-accessible surface bounded molecular volume and van der Waals-surface-bounded molecular volume calculations are based on a grid method derived by Bodor et al., using the atomic radii of Gavezotti.[50,51]

Hydration energy is a key factor determining the stability of different molecular conformations in water solutions.

Log*P* is used to predict the solubility of oral drugs; this is done by partitioning the molecule between water and the hydrophobic solvent *n*-octanol, and determining the *P* value as the ratio of the concentration of the compound in *n*-octanol and that in water. If log*P* increases, solubility in water decreases so absorption decreases. On one hand, a negative value for log*P* indicates that the compound is too hydrophilic. So it has good aqueous-solubility, better gastric tolerance and efficient elimination through the kidneys. On the other hand, a positive value for log*P* indicates that the compound is too lipophilic. So it has a good permeability through a biological membrane, a better binding to plasma proteins, elimination by metabolism but a poor solubility and gastric tolerance.[52]

Compound (8) is expected to have the highest hydrophilicity because of its log*P* value, which implies that this compound will have good aqueous-solubility, better gastric tolerance and efficient elimination through the kidneys whereas compound (17) will be the most lipophilic, this implies that this compound will have good permeability across the cell membrane. We observe that polarizability data are approximately proportional to molecular volume and surface. Compound number 20 shows the maximum value of both polarizability (43.12 Å^3) and this compound has also high values of molecular weight (387.45 amu), volume (1069.86 Å^3) and surface (633.37 Å^2). Compound 14 indicates the maximum absolute value of Hydration energy (12.02 kcal/mol). Regarding compound 17, it shows the minimum absolute value (4.55 kcal/mol). In fact, the hydrophobic majority molecules of thiazolidine-2,4-dione derivatives lead to the decrease of the hydration energy. Contrariwise, the presence of hydrophilic groups in the compound (14), having one (HBD): (1 NH) and seven (HBA): (five O, 1N and 1 S) leads to the increase of the hydration energy.

Energies of the HOMO and LUMO are very popular quantum chemical descriptors. The energy of the HOMO is directly related to the ionization potential and characterizes the susceptibility of the molecule toward attack by electrophiles. The energy of the LUMO is directly related to the electron affinity and characterizes the susceptibility of the molecule toward attack by nucleophiles. Both the HOMO and the LUMO energies are important in radical reactions.[33]

Among the various substitutes that we have added each time to the thiazolidine-2, 4-dione and by the calculations that we have performed, it was found that the compound 2 (5-(4-(2-morpholinoethoxy) benzylidene) thiazolidine-2,4-dione) has the lowest energy gap HOMO-LUMO (0.1315 au), so the compound (2) is predicted to be the most reactive with smaller HOMO–LUMO energy gap of all thiazolidine-2,4-dione derivatives systems.

Quantitative structure-activity relationships studies

In this part, we have studied the correlation of the biological activities with the physicochemical and quantum parameters of the thiazolidine-2,4-dione derivatives.

Multiple linear regressions MLR

Multiple linear regression (MLR) analyses were used to find the relationship between molecular descriptors and inhibition of 15-PGDH activity.

The derived MLR QSAR models are represented by the following equation (1):

$$\text{pIC 50} = -1221.168 - 0.110\ \text{SAG} + 0.050\ \text{MV} - 0.632\ \text{Pol} + 0.403\ \text{HE} + 0.096\ \text{MV} -$$

$$-181.927\ E_{HOMO} + 413.380\ E_{LUMO} + 53.045\ q_{N3} + + 1708.204\ q_{C5} + 786.080\ q_{O7}$$

$$n = 22,\ R^2 = 0.9623,\ R^2_{pred} = 0.7839,\ S = 0.1859,\ F = 13.9250$$

The model fulfills (equation 1) the selection criteria's such as $r^2 > 0.6$ (0.9623) explains 96.2% variance for inhibition of 15-PGDH activity between descriptors (SAG, MV, Pol, HE, MW, E_{HOMO}, E_{LUMO}, q_{N3}, q_{O7}, q_{C5} and q_{C4}), with low standard error of squared correlation coefficient $S < 0.3$ (0.1859) show the relative good fitness of the model and the value of F (13.9250) is greater than tabulated F value show the statistical significance of the regression model, note that the calculated of F is determined with a confidence limit superior to 95% for this model.

In the equation of pIC_{50}, the negative coefficient of SAG explains that any increase in the surface area grid of the compounds causes a decrease in the biological activity, and the positive coefficients of MW and MV explain that any increase in molecular weight and molecular volume of the compounds causes an increase in the biological activity.

It can be observed that high coefficients of atomic charges on atoms C4, O7 and N3 (q_{C4}, q_{O7} and q_{N3} respectively) and coefficients of E_{LUMO}, thus, lead to increasing the inhibition activity of *15-PGDH*.

The charges allowed a physical explanation and electronic molecular properties contributing to inhibition of *15-PGDH* potency as the electronic character related directly to the electron distribution of interacting molecule at the site active.

For validation of the model, we plot in (Fig. 2) the experimental activities against the predicted values as determined by equation (1). We can observe that the predicted pIC_{50} values are in an acceptable agreement and regular distribution with experimental ones with $R^2 = 0.962$ and $R^2_{Pred} = 0.7839$.

As can be seen, the QSAR model has good statistical quality with low prediction error.

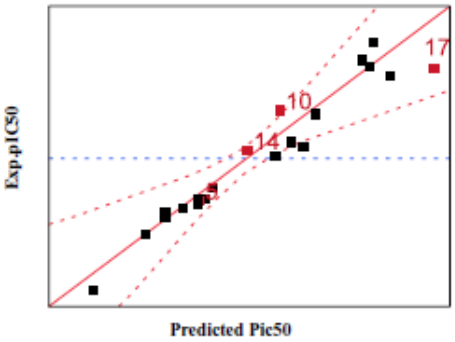

Fig. 2 – Plots of predicted versus experimentally observed *15-PGDH* inhibitor activity using MLR.
Exp. pIC_{50} – experimental values of the biological activity; predicted pIC_{50}: Predicted values of the biological activity.

Artificial neural networks

ANN is artificial system simulating the function of the human brain. Three components constitute a neural network: the processing elements or nodes, the topology of the connections between the nodes, and the learning rule by which new information is encoded in the network. While there are a number of different ANN models, the most frequently used type of ANN in QSAR is the three-layered feed-forward network.[53]

In order to increase the probability of good characterization of studied compounds, artificial neural networks (ANN) can be used to generate predictive models of quantitative structure-activity relationships (QSAR) between a set of molecular descriptors obtained from the MLR, and observed activity. The ANN calculated activities model was

developed using the properties of several studied compounds.[54,55]

In this work, ANN contained eleven inputs corresponding to the eleven descriptors selected from the correlation matrix, three hidden neurons, and one output neuron which is pIC50 (Fig. 3). The number of artificial neurons in the hidden layer were adjusted experimentally,[56] three neurons in the hidden layer were permitted to attain the best correlation between experimental and predicted data. Then, the ANN was trained using the Gauss-Newton method. A good correlation between experimental and predicted pIC50 by ANN is found. This is shown in Fig. 4, and illustrated by R^2 and R^2_{Pred} values of $R^2 = 0.9963$ and $R^2_{Pred} = 0.6324$.

From both results of training and test sets (Fig. 4), we can conclude that the ANN model with (11-3-1) architecture can establish a satisfactory relationship between the eleven descriptors and the inhibition activity of *15-PGDH*. For instance, all test molecules (5, 10, 14 and 17) are in good agreement with the two models.

The predicted activities (MLR, ANN) using by JMP regression method are listed in Table 3.

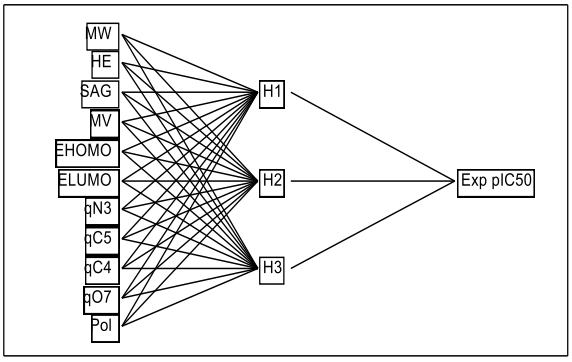

Fig. 3 – Structure of ANN.

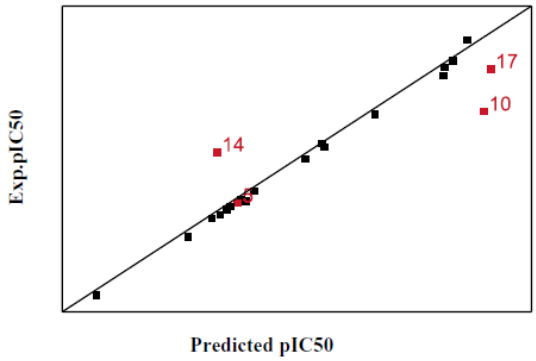

Fig. 4 – Correlation of experimental and predicted pIC50 as calculated by ANN.

Table 3

Experimental and predicted (MLR and ANN) activities of thiazolidine-2,4-dione derivatives

Compounds	pIC50 $_{exp.}$	pIC50$_{pred}$(MLR)	pIC50$_{pred}$(ANN)
1	7.508	7.484	7.388
2	6.146	6.150	6.156
3	7.220	7.230	7.268
4	5.903	5.868	5.917
5	6.180	6.351	6.044
6	5.430	5.519	5.451
7	6.125	6.183	6.129
8	6.200	6.186	6.249
9	6.542	6.555	6.564
10	6.935	6.755	7.281
11	6.050	5.962	6.079
12	6.276	6.256	6.231
13	6.634	6.775	6.605
14	6.598	6.562	6.178
15	7.347	7.345	7.347
16	6.906	6.972	6.930
17	7.283	7.363	7.452
18	6.660	6.738	6.626
19	6.207	6.155	6.181
20	6.090	5.997	6.107
21	6.280	6.280	6.278
22	7.292	7.126	7.308

pIC50 $_{exp.}$ – experimental values of the biological activity;
pIC50 $_{pred.}$ – predicted values of the biological activity (MLR and ANN). The following parameters were carried out using the software JMP 8.0.2[42]

External Validation

To estimate the predictive power of a QSAR model, Golbraikh and Tropsha recommended the use of the following statistical parameters using the test set.[57,58] The predictive abilities of the best MLR and ANN were tested (Table 4) using the Golbraikh-Tropsha criteria and the $R^2_{\text{pred test}}$.

All the calculated parameters indicated the models (MLR and ANN) have good predictive power. Analyzing the results of the external test set listed in Table 3 (which is in red), it could be observed that all the Golbraikh-Tropsha criteria were fulfilled.

Table 4

Predictive power results for the external test set; Golbraikh and Tropsha criteria

Model	R^2_{pred}	K	K'	R^{o2}	R'^{o2}	$(R^2 - R^{o2})/R^2$	$(R^2 - R'^{o2})/R^2$	$\lvert R^{o2} - R'^{o}\rvert$
MLR	0.7839	0.9970	1.0018	0.9989	0.9993	–0.0183	–0.0185	–0.0004
ANN	0.6324	0.9980	1.0001	0.9996	0.9999	–0.0022	–0.0024	–0.0003
	> 0.6	> 0.85	< 1.15	Close to R^2	Close to R^2	< 0.1	< 0.1	< 0.3

$R^2_{\text{pred}}$is the predicted correlation coefficient.
R^{o2} and r'^{o2} are the squared correlation coefficient.
K and K' are the slopes of regression lines through the origin for fits to experimental and predicted data respectively.

The external predictability of the selected model was also checked by r_m as proposed by Roy Paul (2008)[58] and the different r^2_m values were calculated using equations.

The external predictability of the selected model was also checked by concordance correlation coefficient (CCC), as proposed by Gramatica *et al.*[59]

Table 5

Validation characteristics of the developed model according to r^2_m metrics and concordance correlation coefficient

r^2_m parameter			Concordance correlation coefficient
Model	r^2_m	r'^2_m	CCC
MLR	0.7781	0.7771	0.9158
ANN	0.9280	0.9253	0.8765
	> 0.5	> 0.5	> 0.85

r^2_m closeness between the R^2 and R^{o2} determination coefficients
$r^{2'}_m$ closeness between the R^2 and $R^{o'2}$ determination coefficients

All parameters in (Table 5) meet the criteria of r^2_m metrics and concordance correlation coefficient and extend more efficient evidence of external predictability of the generated QSAR.

CONCLUSION

In the present work, we have studied the correlation of the biological activities with the physicochemical and quantum parameters of the thiazolidine-2,4-dione derivatives. Our results suggest a MLR QSAR model based of the following descriptors: HE, POL, SAG, MV, E_{HOMO}, E_{LUMO}, q_{N3}, q_{O7}, q_{C5} and q_{C4} for the specific activity of inhibition of 15-PGDH.

The model MLR fulfills the selection criteria's such as $r^2 > 0.6$ (0.9623) explains 96.2% variance for inhibition of 15-PGDH activity between descriptors (SAG, MV, Pol, HE, MW, E_{HOMO}, E_{LUMO}, q_{N3}, q_{O7}, q_{C5} and q_{C4}), with low standard error of squared correlation coefficient $S < 0.3$ (0.1859) show the relative good fitness of the model

Thus, grace to QSAR studies, especially with the ANN that has allowed us to improve the correlation between the observed biological activity and that predicted, we could enjoy the performance of the predictive power of this model to explore and propose new molecules could be active.

From both results of training and test sets (R^2 = 0.9963 and R^2_{Pred} = 0.6324.), we can conclude that the ANN model with (11-3-1) architecture can establish a satisfactory relationship between the eleven descriptors and the inhibition activity of 15-PGDH.

Furthermore, we can conclude that studied descriptors, which are sufficiently rich in chemical and topological information to encode the structural feature and have a great influence on the

activity may be used with other descriptors for the development of predictive QSAR models.

The model was validated using the external test set.

The QSAR model proposed in this work is expected to be a useful tool in the conception of novel active molecules.

REFERENCES

1. V. S. Jain, D. K. Vora and C. S. Ramaa, *Bioorg. J. Med. Chem*., **2013,** *21*, 1599–1620.
2. M. S. Faiyazalam, B. P. Navin and R. Dhanji, *Indian J. Res. Pharm. Biotechnol.*, **2013,** *1*, 496–503.
3. F. L. Gouveia, R. M. B. Oliveira, T. B. Oliveira, I. M. Silva, S. C. Nascimento, K. X. F. R. Sena and J. F. C. Albuquerque, *Eur. J. Med. Chem.*, **2009,** *44*, 2038–2043.
4. M. Tuncbilek and N. Altanlar, *Arch. Pharm. J. Chem. Life Sci.*, **2006,** *339*, 2132016.
5. R. Murugan, S. Anbazhagan, S. Lingeshwaran and S. S. Narayanan, *Eur. J. Med. Chem.*, **2009,** *44*, 3272–3279.
6. S. R. Pattan, C. Suresh, V. D. Pujar, V. V. K. Reddy, V. P. Rasal and B. C. Koti, *Ind. J. Chem.*, **2005**, *44*, 2404–2408.
7. B. R. Bhattarai, B. Kafle, J. Hwang, D. Khadka, S. Lee, J. Kang, S. W. Ham, I. Han, H. Park and H. Cho, *Bioorg. J. Med. Chem. Lett.*, **2009,** *19*, 6161–6165.
8. A. M. Youssef, M. S. White, E. B. Villanueva, I. M El-Ashmawy and A. Klegeris, *J. Med. Chem.*, **2010**, *18*, 2019.
9. O. Bozdag-Dundar, T. Coban, M. Ceylan-Unlusoy and R. Ertan, *J. Med. Chem. Res.*, **2009**, *18*, 1–7.
10. V. Patil, K. Tilekar, S. Mehendale-Munj, R. Mohan, and C. S. Ramaa, *Eur. J. Med. Chem.*, **2010,** *45*, 4539–4544.
11. N. Shimazaki, N. Togashi, M. Hanai, T. Isoyama, K. Wada, T. Fujita, K. Fujiwara and S. Kurakata, *Eur. J. Cancer,* **2008,** *44*, 1734–1743.
12. B. Donnelly, T. C. Downie, R. Grzeskow, H. R. Hamburg and D. Short, *J. Corros Sci.*, **1974**, *14*, 597–606.
13. N. Aoumeur, N. Tchouar, S. Belaidi, D. Harkati, H. Belaidi and A. Rouane, *Rev. Roum. Chim*., **2019**, *64*, 935–948.
14. J. Weinberg, Dan A. Lerner and C. Bălăceanu-Stolnici, *Rev. Roum. Chim*., **2007**, *52*, 759–764
15. M. Ibrahim and H. Elhaes, *Rev. Theor. Sci.,* **2013,** *1*, 368–367.
16. E. C. Anota, H. H. Cocoletzi and M. Castro, *J. Comput. Theor. Nanosci.*, **2013**, *10*, 2542–2546.
17. A. Vârlan, S. Ionescu, S. H. Suh and M. Hillebrand, *Rev. Roum. Chim*., **2007**, *52*, 733–737
18. Y. C. Martin "Quantitative Drug Design", Marcel Dekker, New York, NY, USA, 1978, p. 1–9.
19. A. Chiriac, D. Ciubotariu, S. Funar-Timofei, L. Kurunczi, M. Mracec, M. Mracec, Z. Szabadai, E. Şeclăman and Z. Simon, *Rev. Roum. Chim*., **2006**, *51*, 79–99
20. P. Gabriel Anoaica, E. Amzoiu and C. I. Lepădatu, *Rev. Roum. Chim*., **2007**, *52*, 789–793.
21. M. Mracec, A. Borota, R. Rad, L. Ostopovici and M. Mracec, *Rev. Roum. Chim*., **2007**, *52*, 829–835
22. M. Mracec, L. Juchel and M. Mracec, *Rev. Roum. Chim*., **2006**, *51*, 287–292
23. A. Hosam, D. Darko and G. Wei, *Can. J. Chem.*, **2017**, *95*, 174–183.
24. F. B. Hershey, G. Johnson, S. M. Murphy and M. Schmidt, *Cancer Res.* ,**1966**, *26*, 257–265.
25. T. T. Otani and H. P. Morris, *J. Natt. Cancer Inst.*,**1971**, *47*, 1247–1254.
26. J. G. Topliss, *Perspect. Drug Discov. Des.*,**1993**, *1*, 253–268.
27. A. Eghdami and M. Monajjemi, *Quantum Matter,* **2013**, *2*, 324–331.
28. S. Medjahed, S. Belaidi, S. Djekhaba, N. Tchouar, and A. Kerassa, *J. Bionanosci.,* **2016**, *10*, 118–126.
29. O. Oukil, N. Tchouar, S. Belaidi, T. Salah and M. Cinar, *Rev. Roum. Chim.*, **2017**, *62*, 81–92.
30. S.K.M. Alam, S. Samanta, A. K. Halder, S. Basu and T. Jha, *Eur. J. Med. Chem.*, **2009**, *44*, 359–364.
31. K. Dermeche, N. Tchouar, S. Belaidi, T. Salah, *J. Bionanosci*., **2015**, *9*, 395–400.
32. S. Belaidi, R. Mazri, H. Belaidi, T. Lanez, D. Bouzidi, *Asian J. Chem.*, **2013**, *25*, 9241–9245.
33. A. Kerassa, S. Belaidi, D. Harkati, T. Lanez, O. Prasad, L. Sinha, *Rev. Theor. Sci*., **2016**, *4*, 85–96.
34. M. Ouassaf, S. Belaidi, K. Lotfy, I. Daoud, H. Belaidi, *J. Bionanosci*., **2018**, *12*, 26–36.
35. Z. Almi, S. Belaidi, L. Segueni, *Rev. Theor. Sci*., **2015**, *3*, 264–272.
36. V. Guillén-Casla, N. Rosales-Conrado, M.E. León-González, L.V. Pérez-Arribas and L.M. Polo- Díez, *J. Food Compos. Anal*., **2011**, *24*, 456–464.
37. L. Douali, D. Villemin and D. Cherqaoui, *J. Chem. Inf. Comput. Sci*., **2003**, 43, 1200–1207.
38. H. TaiH, C.M Ensor, Z. Huiping and Y. Fengxiang, "Structure and Function of Human NAD+ –Linked 15-Hydroxyprostaglandin Dehydrogenase, in Eicosanoids and Other Bioactive Lipids in Cancer, Inflammation, and Radiation Injury", 5, K. V. Honn (Ed.), Springer US, Boston, MA, 2002, pp. 245–250.
39. H. Cho, *Appl. Chem.*, **2006**, *10*, 196.
40. L. Wei, X. Yu, H. Shi, B. Zhang, M. Lian, J. Li, T. Shen, Y. Xing and D. Zhu, *Cell. Signal.*, **2014**, *26*, 1476.
41. J. F. Michelet, L. Colombe, B. Gautier, O. Gaillard, F. Benech, R. Pereira, C. Boulle, M. Dalko-Csiba, R. Rozot, M. Neuwels and B. Bernard, *Exp. Dermatol.*, **2008**, *17*, 821.
42. J. L. Wallace, *Physiol. Rev*., **2008,** *88*,1547.
43. O. Belal Al-Najjar, K. Ashok Shakya, F. Saqallah, *Indian J. Chem.*, **2017**, *56B*, 1200–1206
44. Y. Wu, H. H. Tai and H. Cho, *J. Bioorg. Med. Chem.*, **2010,** *18*, 1428–1433.
45. HyperChem (Molecular Modeling System) Hypercube, Inc., 1115 NW, 4th Street, Gainesville, FL 32601, USA, 2008.
46. M. J. Frisch, G. W. Trucks, H. B. Schlegel, G. E Scuseria, M. A. Robb, J. R. Cheeseman, G .Scalmani, V. Barone, B. Mennucci, G. A. Petersson, H. Nakatsuji, M. Caricato, X. Li, H. P. Hratchian, A. F. Izmaylov, J. Bloino, G. Zheng, J. L. Sonnenberg, M. Hada, M. Ehara, K. Toyota, R. Fukuda, J. Hasegawa, M. Ishida, T. Nakajima, Y. Honda, O. Kitao, H. Nakai, T. Vreven, J. A. Montgomery, J. E. Peralta, F. Ogliaro, M. Bearpark, J. J. Heyd, E. Brothers, K. N. Kudin, V. N. Staroverov, T. Keith, R. Kobayashi, J. Normand, K. Raghavachari, A. Rendell, J. C. Burant, S. S. Iyengar, J. Tomasi, C. M. Cossi, N. Rega, J. M. Millam, M. Klene, J. E. Knox, J. B. Cross, V. Bakken, C. Adamo, J. Jaramillo, R. Gomperts, R. E. Stratmann, O. Yazyev, A. Austin, R. Cammi, C. Pomelli, J. W. Ochterski, R. L. Martin, K. Morokuma, K. Zakrzewski, G. A. Voth, P. Salvador, J. J. Dannenberg, S. Dapprich, A. D. Daniels, O. Farkas, J. B. Foresman, J. V. Ortiz, J. Cioslowski and D. J. Fox, Gaussian 09, Gaussian Inc. Wallingford. CT, 2010.

47. JMP 8.0.2, SAS Institute Inc., 2009.
48. MarvinSketch 6.2.1 (2014), Chemaxon (http://www.chemaxon.com).
49. A. Gavezzotti, *J. Am. Chem. Soc.*,**1983,** *105*, 5220–5225.
50. J. Chen-Wei, Z. Xiang, X. Rui-Hua and L. Fu-Li, *Quantum Matter*, **2013**, *2*, 353–363.
51. S. Schultes, C. Graaf and E. Haaksma, *J. Drug Discov. Today: Technologies*, **2010**, *7*, 157–162.
52. V. J. Zupan and J. Gasteiger, "Neural Networks for Chemists – An Introduction", VCH Verlagsgesellschaft, Weinheim/VCH Publishers, New York, 1993, p. 1367–1368.
53. S. S. So and W. G. Richards, *J. Med. Chem.*, **1992**, *35*, 3201–3207.
54. T. A. Andrea and H. Kalayeh, *J. Med. Chem*., **1991**, *34*, 2824–2836.
55. M. Larif, A. Adad, R. Hmammouchi, A. I. Taghki, A. Soulaymani, A. Elmidaoui, M. Bouachrine and T. Lakhlifi, *Arab. J. Chem*., **2017**, *10*, 946–955.
56. A. Golbraikh and A. Tropsha, *Mol. Divers*., **2000**, *5*, 231–243.
57. L. Sachs, "Statistics: A Handbook of Techniques", Springer-Verlag, Berlird, New York, 1984.
58. P. P. Roy, S. Paul, I. Mitra and K. Roy, *Molecules*, **2009,** *14*, 1660–1701.
59. N. Chirico and P. Gramatica, *J. Chem. Inf. Model*., **2012**, *52*, 2044–2058.